MATEC Web of Conferences **22**, 02032 (2015)
DOI: 10.1051/matecconf/20152202032

Optimum Design for Slot-type of Stator Based on PM Motor with Halbach Structure

Yongxin Zhu* & Mingzhong Qiao
College of Electric Engineering, Naval University of Engineering, Wuhan, Hubei, China

ABSTRACT: The performance of permanent magnet motor is directly influenced by the PM structure of rotor and the slot type of stator. An emerging rotor magnetization type of PM motor is Halbach structure, which has obvious advantages in comparison to ordinary permanent structures and in application, especially in the design of propeller integration system. Commonly, Halbach array is used in discrete permanent magnet structure on the rotor of machine. On the stator, air gap flux density varies as the slot type changes, and complex slot types will bring about complex air gap equivalent process of the motor, which will influence the procedures of simulation calculation and experiments. According to the characteristics of Halbach array, the intensifying effect of the Halbach array on magnetic flux density of air gap is analyzed in this paper, and the electromagnetic field of PM motor is calculated. By using FEM method, the magnetic flux density of air gap, back phase electromotive force and electromagnetic torque are compared under different slot types. Simulation result shows the peer slot is best. Experiments on a 60kW PM Motor with Halbach Structure and peer slot is in good agreement with simulation.

Keywords: PM motor; stator slot-type; air-gap magnetic flux density; torque-ripple

1 INTRODUCTION

Increasing the air-gap flux density of motor is effective in reducing motor size and increasing energy density [1]. Generally there are two approaches. One is to choose materials with high residual magnetic flux density. The other is to change the arrangement of magnetic-steel structure. Researcher Klaus Halbach from Lawrence Berkeley National Lab in the U.S. created the Halbach array in 1979, which provided an excellent solution to the second approach.

The original study on Halbach array started with the development of propeller integration system. Common PM motor can't meet the needs of propeller integration system because of the limits to motor size, weight and air-gap width. As the Halbach array has optimal effect on rotor poles, the requirements of propeller integration PM motor can be properly adapted by using this array. As a result, the development of propeller integration motor is greatly promoted. Consequently, Halbach arrays are widely used in different fields, such as high-speed motor, servo motor and medical science.

A large amount of theoretical and application study has been made on Halbach array. References [2] and [3] built Halbach array magnetic field model by using magneto-motive force method, under the condition of unlimited length of PM structure. Reference [4] presented that the thickness of PM structure has apparent influence on air-gap flux density. Reference [5] studied motor dynamic procedures by using magnetic circuit method. Reference [6] put forward that for out-rotor Halbach motors the proportion of inner diameter and outer diameter is an important factor affecting air-gap flux density. Reference [7] compared the performances of traditional spherical motors and Halbach spherical motors by using FEM method. Reference [8] superposed magnetic fields produce by single PM steels, but calculation amount is too big. All these studies have acquired fine academic achievements, but few researches have concerned the relationship between the stator of PM motor and air-gap flux density. In fact, the structure of stator will apparently influence the air-gap flux density.

According to the characteristics of Halbach array, the intensifying effect of the Halbach array on magnetic flux density of air-gap is analyzed, and the electromagnetic field of PM motor is calculated. By using FEM method, the magnetic flux density of air-gap, back phase electromotive force and electromagnetic torque are compared under different slot-types.

2 HALBACH ARRAY

2.1 *Halbach structure*

In general, radial or tangential structure is used on a PM motor. Halbach array combines two structures together. The auxiliary tangential magnet can weaken magnetic flux leakage between poles, and compensate main pole flux because of superposition. As a result of combination, the magnetic field intensity of one side is very strong while that of the other side is very weak, as is shown in Figure 1. By making use of this feature, the dynamic control characteristics of motor will be increased or the air-gap width can be increased without decreasing the amplitude of air-gap flux density, which will certainly improve the reliability of the motor.

*Corresponding author: gagaga92@163.com

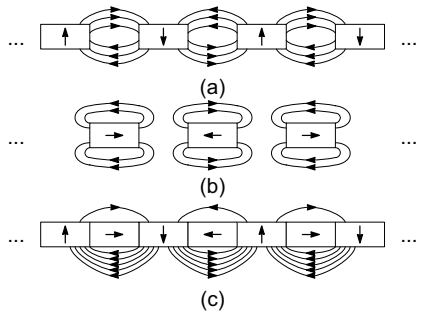

(a) Radial structure (b) Tangential structure (c) Halbach Array

Figure 1. Halbach array structure

2.2 *Features of Halbach array*

Halbach array has many excellent characteristics:

(1) Halbach array may produce ideal sinusoidal distributed magnetic field in space, which can apparently reduce cogging-torque.

(2) Halbach structure has strong magnetic field on one side and weak magnetic field on the other side. This may help to improve air-gap flux density and power density, to reduce size and yoke flux.

(3) High magnetic energy density can allow the motor to have wide air-gap. Halbach array can increase motor efficiency and reduce open circuit loss.

(4) By using Halbach array, torque ripple can be decreased and the requirements of the motor for the bearing can also be decreased.

Figure 2 shows the composition of magnetic force line, which intuitively reflects the optimizing effect of Halbach structure on air-gap.

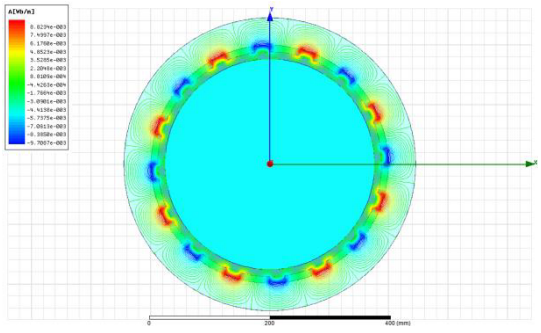

Figure 2. Halbach motor air-gap magnetic field

3 MAGNETIC FIELD ANALYSIS OF HALBACH MOTOR

3.1 *Magnetic circuit analysis for PM motor*

During the operating process, magnetic force Fm and flux φ_m in outer circuit produced by PM structure is variable. PM structure is equivalent to a parallel connection source including a constant flux source φ_r and a constant magnetic conductance $\wedge_0$, as is shown in Figure 3.

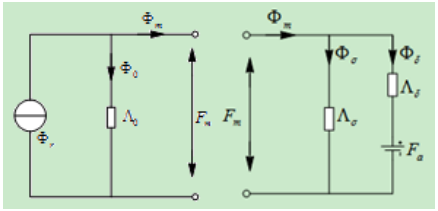

Figure 3. PM motor equivalent magnetic circuit

In Figure 3, φ_m is the total flux per pole (Wb) provided from PM structure to outer magnetic circuit; φ_r is virtual intrinsic flux, which is a constant under given performance and size of PM structure; φ_0 is virtual leakage flux of PM, $\wedge_0$ is the inner magnetic conductance(H) of PM, which is also a constant under given performance and size of PM structure; Fm is the outer magnetic circuit magneto-motive force produced by both PM ends of each pair of poles(A).

The total flux φ_m can be divided into two parts: one is main flux (air-gap flux per pole) φ_δ, and the other is leakage flux φ_σ. Accordingly, outer magnetic circuit can be divided into main circuit and leakage circuit, and the corresponding magnetic conductance are main conductance Λm and leakage conductance $\wedge_\sigma$. Assuming that when the motor operates, armature magneto-motive force Fm produced by every pair of poles' circuit contains both direct axis and quadrature axis magneto-motive force, the equivalent circuit is shown in Figure 3. The value of Fm is positive during demagnetization, otherwise negative. The whole equivalent magnetic circuit is the combination of Figure 3(a), (b).

3.2 *Electromagnetic analysis for PM motor*

Considering the complexity in the real manufacturing process, a discrete 90º Halbach structure is often used in engineering. According to the research, taking 2:1 as the proportion of radial and tangential PM size can properly trade off between air-gap flux density, approximate sinusoidal distribution, and limits of manufacturing process [9]. In order to reduce the calculation workload, the common rectangular coordinate system should be changed [10]. Figure 4 shows the calculation model of the motor magnetic field, where Rr is inner diameter of PM structure; Rm is outer diameter of PM structure; Rs is inner diameter of the stator; τ_{mp} is pole distance; τ_{mr} is the arc length of radial magnet; $\tau_{m\theta}$ is the arc length of tangential magnet; β is the ratio coefficient, i.e., $\tau_{mr} / \tau_{m\theta}$.

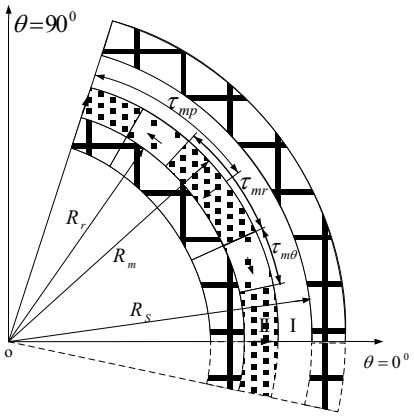

Figure 4. 90º Halbach motor structure

According to the principle of flux continuity $\nabla \cdot \vec{B} = 0$, the basic magnetic field equation in area I and II can be deducted

$$\nabla^2 \varphi_{\mathrm{I}} = \frac{\partial^2 \varphi_{\mathrm{I}}}{\partial r^2} + \frac{\partial \varphi_{\mathrm{I}}}{r \partial r} + \frac{\partial^2 \varphi_{\mathrm{I}}}{r^2 \partial \theta^2} = 0$$

$$\nabla^2 \varphi_{\mathrm{II}} = \frac{\partial^2 \varphi_{\mathrm{II}}}{\partial r^2} + \frac{\partial \varphi_{\mathrm{II}}}{r \partial r} + \frac{\partial^2 \varphi_{\mathrm{II}}}{r^2 \partial \theta^2} = \frac{\nabla \vec{M}}{\mu_r}$$

$$\nabla \vec{M} = \frac{M_r}{r} + \frac{\partial M_r}{\partial r} + \frac{\partial M_\theta}{r \partial \theta} \tag{1}$$

In polar coordinates,

$$\vec{M} = M_r \vec{e}_r + M_\theta \vec{e}_\theta \tag{2}$$

Where, M is the residual magnetization of PM; Mr and $M\theta$ are respectively the radial and tangential component of M. The existence of M makes the equation non-homogeneous.

In discrete Halbach array, the changes of Mr and $M\theta$ are not continuous. Fourier series should be used to decompose Mr and $M\theta$ so as to obtain the divergence of M. In practice, the calculation of air-gap magnetic field should consider variations produced by rated excitation in stator winding.

4 ANALYSIS OF DIFFERENT SLOT-TYPE ON MAGNETIC FIELD OF HALBACH MOTOR

According to the above-mentioned analysis, when the structures of stator and rotor are given, the air-gap flux is closely related to stator slot-type. Based on a 3-phase PM motor (basic parameters are shown in Table 1), the phase back electromotive force under rated rotating speed and the torque-ripple under rated operating state are compared between different slot types, i.e., open-square slot, peer slot and trapezoidal slot. The sizes of different slot types are in accordance with space factor.

Table 1. Motor parameter

Parameter	Value	Parameter	Value
Rated power	60kW	Number of turns in series per phase	88
Rated line voltage	380V	Stator teeth distance	13.4mm
Pair of poles	8	Rated phase current	101A
Number of slots	96	Rated speed	975r/min
Outer diameter of stator	490mm	Copper space factor	0.7484
Inner diameter of stator	410mm	Stator yoke height	11.3mm
Outer diameter of rotor	398mm	Polar distance	80.5mm
Air-gap width	6mm	Pole-arc coefficient	0.70
Conductors per slot	22	Paraller branches	4
Core length	115mm	PM height	11mm
Winding pitch	6	Stacking factor	0.93
Stator DC resistance	0.068ohm	Insulating paint thick	0.08mm

The stator uses double-layer winding; residual magnetic steel is 1.18T; the coercive is 891A/m. The stator and rotor are built with silicon steel sheet, with type DW465_50.

The effective areas of three different slot types are of the same. Ansoft software is used for modeling and simulation. The specifications of different slot types, as is shown in Figure 5, are defined as follows:

(a) Open-square slot: bottom length b=7.19mm, height between bottom line and slot notch h=28.7mm;

(b) Peer slot: notch height h1=1mm, circular arc radius of stator notch r1=3.6mm, height between stator inner diameter and bottom circle center h2=18.62mm, stator notch width b1=3.6mm, stator bottom circular arc radius r2=5.48mm;

(c) Trapezoidal slot: notch height h1=1mm, slot shoulder height h2=2mm, height between shoulder and bottom h3=25.7mm, notch width b1=3.6mm, shoulder width b2=7.2mm, slot bottom width b3=8.026mm.

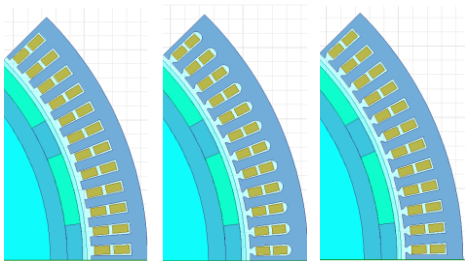

(a) (b) (c)

Figure 5. Slot size

4.1 *Wave form of air-gap flux*

According to Fourier transform of equation (1), the air-gap radial and tangential flux of PM motor can be described as follows:

$$B_{1r} = -\sum_{n=1}^{\infty} \frac{B_r}{\Delta_0} \frac{np}{1-n^2p^2} \Delta_1 [(\frac{r}{R_s})^{np-1} (\frac{R_m}{R_s})^{np+1} + (\frac{R_m}{r})^{np+1}] \cos(np\theta)$$

$$B_{1\theta} = \sum_{n=1}^{\infty} \frac{B_r}{\Delta_0} \frac{np}{1-n^2p^2} \Delta_1 [(\frac{r}{R_s})^{np-1} (\frac{R_m}{R_s})^{np+1} - (\frac{R_m}{r})^{np+1}] \sin(np\theta) \quad (3)$$

Among three slot types, the peer slot and the trapezoidal slot has bigger radial component of air-gap flux, with a value of 0.77T, while that of the open-square slot is smaller, which can be seen in Figure 6.

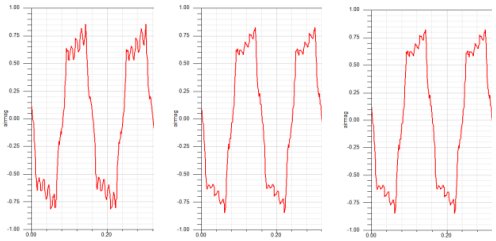

(a) (b) (c)

Figure 6. Air-gap radial flux

4.2 *Phase back electromotive force*

The phase back electromotive force E1 in stator winding is inducted by no-load air-gap fundamental flux produced by PM structure.

$$E_1 = 4.44 f N \phi K_{dp} \quad (4)$$

Where, f is frequency; N is number of turns in series per phase; φ is flux; Kdp is winding coefficient. E1 significantly affects the steady state performance of motor. An appropriate design may raise the working efficient and reduce the temperature of motor.

Open-square slot (a): the effective value of phase back electromotive force is 225.66V, and the effective value of 130Hz fundamental wave is 224.83V. Peer slot (b): the effective value of phase back electromotive force is 233.41, and the effective value of 130Hz fundamental wave is 232.41V. Trapezoidal slot(c): the effective value of back electromotive force is 229.75V and the effective value of 130Hz fundamental wave is 228.97V, as is shown in Figure 7.

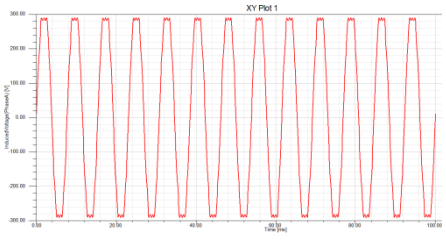

(a)

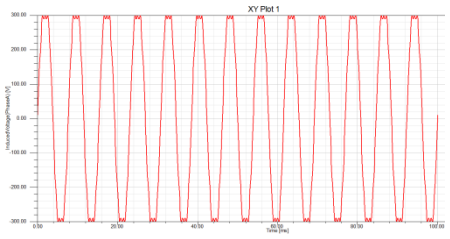

(b)

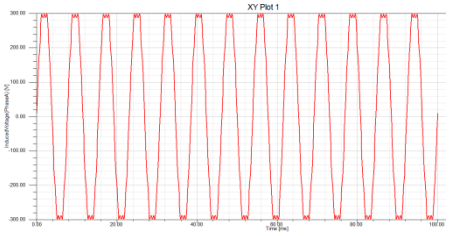

(c)

Figure 7. Phase back electromotive force

The following data is acquired from the results of FFT:

Open-square slot (a): fundamental amplitude of back electromotive force is 317.6V; amplitude of third harmonic wave is 24.9V. Peer slot (b): fundamental amplitude of back electromotive force is 328.3V; amplitude of third harmonic wave is 27.5V. Trapezoidal slot (c): fundamental amplitude of back electromotive force is 323.4V; amplitude of third harmonic wave is 22.9V, as is shown in Figure 8.

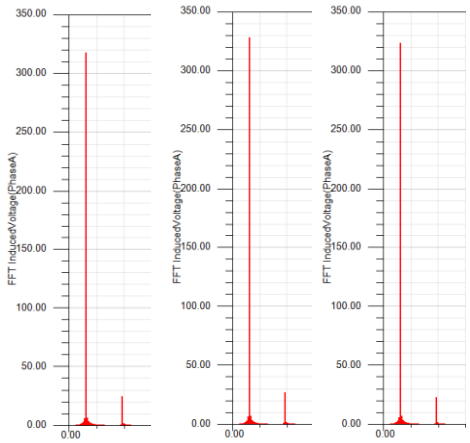

(a) (b) (c)

Figure 8. Phase back electromotive force FFT

4.3 *Electromagnetic torque*

In the two-dimension magnetic field, the density of tangential electromagnetic force working on motor

stator and rotor can be described as

$$f_t = \frac{B_n B_t}{\mu_0} \tag{5}$$

Electromagnetic torque is produced by tangential force. If we do integral around a circle with radius r, the electromagnetic torque is

$$T_{em} = \frac{L_{ef} \oint r^2 B_r B_\theta d\theta}{\mu_0} \tag{6}$$

Where, r is the radius of air-gap circle; Br is the radial component of air-gap flux at radius r; $B\theta$ is the corresponding tangential component. In the circular integral, if radius is defined, then r is a constant. L_{ef} is calculating length of armature; μ_0 is the magnetic conductivity in space.

After adding rated excitation on stator winding, the average torque value of open-square slot (a) is 718.1N/m, with an error of 4.1%. For the peer slot (b), the average is 703.7N/m, with an error of 4.4%. For the trapezoidal slot (c), the average is 698.9N/m, with an error of 4.1%, as is shown in Figure 9.

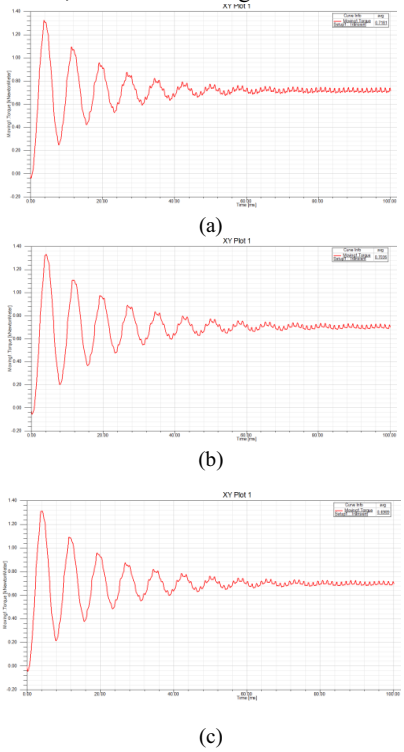

(a)

(b)

(c)

Figure 9. Rated operating torque

In conclusion, motors with different slot types have their own features. Back electromotive force harmonic wave, torque-ripple and transient time cannot be taken into account at the same time. In general, though the PM motor with open-square slot has smaller torque-ripple, the PM motor with peer slot is better as a whole. Based on this, a Halbach PM motor with peer slot is independently developed for experiment and validation.

5 EXPERIMENT

A 60kW Halbach PM motor with peer slot is developed, as is shown in Figure 10. Drive the motor to its rated speed 975rpm, measure the line back electromotive force of ab and ac phases. The waveform is shown in Figure 10 (c). Its effective value are 401V and 402V, which are in good agreement with the conversion results in the simulation and show the validity of simulation results.

(a) Rotor PM (b) Stator winding

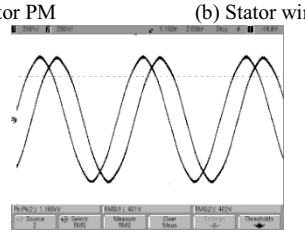

(c) Line back electromotive force

Figure 10. Experiment of 60kW Halbach PM motor with peer slot

Table 2 shows the parameters measured for the motor under rated load operation. The parameter values of the first group are taken from room temperature operation, and those of the second group are from a steady temperature of the motor. Data show that the operation efficiency becomes bigger and power becomes smaller as temperature rises. In general, the performance doesn't change much.

Table 2. Experiment stats

Parameter	Value 1	Value 2
Frequency	130Hz	130Hz
Effective line volt	401V	400V
Effective phase current	91.7A	91A
Input power	63.7kw	63.3kw
Output power	60kw	59.7kw
Efficient	94.19%	94.31%
Power factor	0.9996	0.9987
Temperature	25℃	67℃

6 CONCLUSION

The features and advantages of Halbach array are analyzed, and the electromagnetic field of the motor is calculated. Halbach PM motors with different slot types are simulated and the following results are obtained:

(1) Motors with peer slot and trapezoidal slot have bigger radial component of air-gap flux amplitude, while that for open slot is smaller.

(2) The harmonics of phase back electromotive force mainly focus on third harmonic waves. The effective values of fundamental wave and whole wave for back electromotive force under open circuit are almost of the same for a single slot type. But the fundamental amplitudes for different slot types are obviously different. The peer slot has biggest fundamental amplitude, with a value of 328.3V, while the second is open slot, with a value of 323.4V. For the third harmonics, the open slot and the trapezoidal slot have similar values, and the peer slot is bigger, with a value of 27.5V.

(3) Each slot type has similar transient times, but the open slot comes to steady state 20ms faster than other slot types. The average torques for motors with different slot types are close, with the open-square slot a little bigger, with a value of 718N/m. Considering motor stability, the steady state errors of torque-ripples for three types of slot are all near 4%, which is acceptable.

Motors with different slot types have different air-gap flux density, phase back electromotive force, torque. According to the results, peer-slot motor works better. Consequently, by using an independently developed 60kW Halbach PM motor with peer-slot, experiment shows that the motor works stably.

REFERENCES

[1] Tang Ren-yuan. 1997. *Modern Permanent Magnet Machines Theory and Design*. Beijing: China Machine Press.

[2] Jin P. 2013. General analytical method for magnetic field analysis of Halbach magnet arrays based on magnetic scalar potential. *Journal of Magnetics*, 18(2): 95-104.

[3] Nguyen V H. 2013. A multi-axis compact positioner with a 6-coil platen moving over a superimposed Halbach magnet matrix.

[4] Chen Chuican, Ji Wenchen, Wang Aijun. 2010. The Effect of Magnet Structure Size on Halbach Array. *Electric Switch Gear*, 6(4): 11-13.

[5] Liu Y. 2011. Optimization of voice coil motor to enhance dynamic response based on an improved magnetic equivalent circuit model. *IEEE Transactions on Magnetics*, 47(9): 2247-2251.

[6] Johnson D, Pillary P, Malengret M. 2001. High speed PM motor with hybrid magnetic bearing for kinetic energy storage. *IEEE Industry Applications Conference*, (1): 57-63.

[7] Hongfeng Li, Changliang Xia, Peng Song. 2007. Magnetic field analysis of a Halbach array PM spherical motor. *IEEE International Conference on Automation and Logistics*, Shandong, 2019-2023. X

[8] Ham C. 2013. Study of a Hybrid magnet array for an electrodynamic magnet control. *Journal of Magnetics*, 18(3): 370-374. Z

[9] Li Geng, Qiao Mingzhong, Liang Jinghui, Huang Liuwei. 2012. Optimum Design for Halbach Structure Applying Permanent Magnet Motor. *Electric Machines & Control Application*, 39(1): 6-10.

[10] Dwari S, Parsa L. 2011. Design of Halbach array based permanent magnet motors with high acceleration. *IEEE Transactions on Industrial Electronics*, 58(9): 3768-3775.

[11] Zhu Z Q, Xia Z P, Atallah K. 2002. Comparison of Halbach magnetized brushless machines having discrete magnet segments of single ring magnet. *IEEE Transactions on Magnetics*, (9): 2997-2999.